miRNA-seq analysis in skeletal muscle of chicken and function exploration of miR-24-3p

Pengfei Wu [*,†] Mingliang He,[*,†] Xinchao Zhang,[*,†] Kaizhi Zhou,[*,†] Tao Zhang,[*,†] Kaizhou Xie,[*,†] Guojun Dai,[*,†] Jinyu Wang,[*,†] Xinglong Wang,[*,†] and Genxi Zhang[*,†,1]

[*]*College of Animal Science and Technology, Yangzhou University, Yangzhou 225009, China; and* [†]*Joint International Research Laboratory of Agriculture & Agri-Product Safety, Yangzhou University, Yangzhou 225009, China*

ABSTRACT The regulation of skeletal muscle growth and development in chicken is complex. MicroRNAs (**miRNAs**) have been found to play an important role in the process, and more research is needed to further understand the regulatory mechanism of miRNAs. In this study, leg muscles of Jinghai yellow chickens at 300 d with low body weight (slow-growing group) and high body weight (fast-growing group) were collected for miRNA sequencing (**miRNA-seq**) and Bioinformatics analysis revealed 12 differentially expressed miRNAs (**DEMs**) between the two groups. We predicted 150 target genes for the DEMs, and GO and KEGG pathway analysis showed the target genes of miR-24-3p and novel_miR_133 were most enriched in the terms related to growth and development. Moreover, networks of DEMs and target genes showed that miR-24-3p and novel_miR_133 were the 2 core miRNAs. Hence, miR-24-3p was selected for further functional exploration in chicken primary myoblasts (**CPMs**) with molecular biology technologies including qPCR, cell counting kit-8 (**CCK-8**), 5-ethynyl-2'-deoxyuridine (**EdU**) and immunofluorescence. When proliferating CPMs were transfected with miR-24-3p mimic, the expression of cyclin dependent kinase inhibitor 1A (**P21**) was up-regulated and both CCK-8 and EdU assays showed that the proliferation of CPMs was inhibited. However, when the inhibitor was transfected into the proliferating CPMs, the opposite results were found. In differentiated CPMs, transfection with miR-24-3p mimic resulted in up regulation of MYOD, MYOG and MYHC after 48 h. Myotube areas also increased significantly compared to the mimic negative control (**NC**) group. When treated with inhibitor, differentiation CPMs produced the opposite effects. Overall, we revealed 2 miRNAs (novel_miR_133 and miR-24-3p) significantly related with growth and development and further proved that miR-24-3p could suppress the proliferation and promote differentiation of CPMs. The results would facilitate understanding the effects of miRNAs on the growth and development of chickens at the post-transcriptional level and could also have an important guiding role in yellow-feathered chicken breeding.

Key words: growth and development, miRNA-seq, chicken primary myoblasts, proliferation and differentiation, skeletal muscle

INTRODUCTION

Chicken meat has the characteristics of high protein, low fat, and low calorie and it has become a source of high-quality protein for diet (Ren et al., 2018). Yellow-feathered broilers are local poultry breeds in China, and they generally have a unique flavor and better meat quality compared with the white-feathered broilers (Jiang et al., 2019; Wang et al., 2019). Production of yellow-feathered broiler is increasing each year in China and was almost comparable to that of white-feathered broiler in the last two years (Jiang et al., 2018). However, the muscle yield, growth rate and feed efficiency of yellow-feathered broilers are inadequate and still have a great potential for improvement. Therefore, it is very important to explore the regulatory mechanisms of muscle growth and development to solve those problems.

At present, some researches have been performed for chicken muscle development, but most focused on mRNAs. Some of them promote muscle development including myogenic regulatory factors (**MRFs**) (Mok et al., 2015), insulin-like growth factor 1/insulin-like growth factor 1 receptor (**IGF-I/IGF-IR**) (Trouten-

Radford et al., 1991; Roelfsema et al., 2018; Saneyasu et al., 2019), paired box 7 (**PAX7**) (Kansal et al., 2019) and myocyte enhancer factor 2 family (**MEF2**) (Ouyang, et al., 2020), while others inhibit skeletal muscle growth such as myostatin (**MSTN**) (Liu et al., 2016). Studies have also revealed that noncoding RNAs are also very important. MicroRNAs (**miRNAs**) are small noncoding RNAs of about 20 nt that can modulate gene expression at the post-transcriptional level either by inhibiting messenger RNA (**mRNA**) translation or by promoting mRNA degradation (Correia de Sousa et al., 2019). In this way, miRNAs play important roles in regulating a large number of biological and metabolic processes, including cell growth, proliferation, differentiation, and cell death (Liu et al., 2014; Saliminejad et al., 2019; Sun et al., 2019). The first miRNA Lin-4 was discovered by Lee et al. (1993) and Wightman et al. (1993) in the study of *Caenorhabditis elegans.* However, it did not attract the attention of the scientific community until Reinhart et al. (2000) discovered the second miRNA (let-7) 7 y later. Since then, the research on the regulation of miRNAs has been revealed and thousands of miRNAs have been found in various animals and plants.

In recent years, some studies on the regulation of miRNAs in chicken skeletal muscle growth have emerged. Shi and Sun (2017) identified a SNP rs16681031 (+60 C>G) of the pre-miR-1658 gene in the Gushi-Anka chicken population by MassArray matrix-assisted laser desorption/ionization-time of flight mass spectrometry. The SNP was not only significantly associated with body weight at the age of 6, 8, 10, 12 wk, respectively, but also significantly related to the breadth of the chicken chest, body slanting length, and pelvic breadth at 4 wk, chest depth at 8 wk of age, and body slanting length at 12 wk ($P < 0.05$), respectively. Recently, Cao et al. (2020) confirmed that miR-99a-5p significantly promotes proliferation and inhibits myotube formation of skeletal muscle satellite cells by directly targeting the 3' untranslated region (**UTR**) of myotubularin-related protein 3 (**MTMR3**). Huang et al. (2019) found that miR-146b-3p, directly suppressing (phosphatidylinositol 3-kinase, putative) PI3K/(serine/threonine kinase 1) AKT pathway and MyoD family inhibitor domain containing (**MDFIC**), acts in the proliferation, differentiation, and apoptosis of myoblast isolated from the leg muscles of 11-embryo-age chicken.

RNA sequencing (**RNA-Seq**) is a high-throughput technology used to provide a comprehensive view of the transcriptome. In recent years, it has been used to identify new miRNAs for chickens. Fu et al. (2018) identified 92 significant differentially expressed miRNAs from four small RNA libraries of breast muscle tissues for Gushi chicken and Jebessa et al. (2018) performed RNA-seq to analyze differentially expressed miRNAs and mRNAs for skeletal muscle (leg muscle) of embryonic chicks. They identified two miRNA-mRNA interaction networks (miRNA-222a and CPEB3, miRNA-126 and FGFR3) and successfully confirmed these targeting relations experimentally.

Leg muscle is one of the most important parts of skeletal muscle in chicken. In this study, we collected leg muscles of female Jinghai yellow chickens with different bodyweight for miRNA sequencing (**miRNA-seq**). Bioinformatic analysis was used to find differentially expressed miRNAs (**DEMs**). Among them, we further studied the function of miR-24-3p to clarify its role in myogenesis of chicken. These results facilitate understanding the effects of miRNAs on the growth and development of chickens at the post-transcriptional level and could have an important guiding role in Jinghai yellow chicken breeding.

MATERIALS AND METHODS

Animals and Tissues

Female Jinghai yellow chickens used in the study were obtained from Jiangsu Jinghai Poultry Industry Group Co., Ltd. (Nantong City, Jiangsu Province, China). The birds had access to feed and water ad libitum. At 300 d we selected 3 healthy individuals with low body weight (slow-growing [S1, S2, S3]) and 3 healthy individuals with high body weight (fast-growing [F4, F5, F6]) in a population for experiment. All chickens were executed by carotid artery bloodletting after being anesthetized by intravenous injection of 8 mg/kg Xylazine Hydrochloride (X-1251, SIGMA, Japan). The whole leg muscles were then collected immediately, snap-frozen in liquid nitrogen, and stored at −80°C for RNA extraction.

The Construction of cDNA Library and Sequencing

The total RNA was extracted with Trizol (TIANGEN, Beijing, China). The purity, concentration and integrity of RNA samples were tested using a NanoPhotometer spectrophotometer (IMPLEN, CA) and an RNA Nano 6000 Assay Kit of the Agilent Bioanalyzer 2100 system (Agilent Technologies, CA).

Amount of 3 µg total RNA per sample was used to construct the library for sequencing.

First, the 3′ small RNA and 5′ small RNA adaptors were ligated followed by strand synthesis. Products were amplified by PCR and size selected by polyacrylamide gel electrophoresis. Finally, PCR products were purified (AMPure XP system) and library quality was assessed.

The clustering of the index-coded samples was performed on a cBot Cluster Generation System using TruSeq PE Cluster Kit v4-cBot-HS (Illumia) according to the manufacturer's instructions. After cluster generation, the library preparations were sequenced on an Illumina 2500 platform and 150bp single-end reads were generated.

Quality Control and miRNA Analysis

Clean data (clean reads) were obtained by removing reads containing ploy-N and low-quality reads from raw

data. And reads were trimmed and cleaned by removing the sequences smaller than 18 nt or longer than 30 nt. At the same time, Q30 of the clean data were calculated.

The clean data were mapped to the chicken reference sequence (Gallus_gallus-5.0) using Bowtie (Langmead et al., 2009) and miRDeep2 (Friedländer et al., 2012) was used to identify the novel miRNAs. miRNA expression levels were estimated for each sample and normalized by the TPM algorithm (Li et al., 2010). Differential expression analysis was performed using the DESeq2 R package (1.10.1). miRNAs with $P \leq 0.05$ found by DESeq2 were assigned as DEMs.

Target Gene Functional Annotation

Target genes of DEMs were predicted by miRanda (v3.3a) (Betel et al., 2008). Gene Ontology (**GO**) enrichment analysis of the target genes was implemented by the GOseq R packages. We used KOBAS (Mao et al., 2005) software to test the statistical enrichment of differential expression genes in **KEGG** (Kyoto Encyclopedia of Genes and Genomes) pathways.

Analysis of Hub Genes and miRNAs

We first predicted the interactions between all target genes based on the STRING database (Franceschini et al., 2013). We imported the interactions into the software Cytoscape (3.6.1) and used the plug-in Cytohubba to find the hub genes with the Maximal Clique Centrality (**MCC**) method and find the corresponding miRNAs.

Validation of DEMs by qPCR

We re-selected 6 fast- and slow-growing Jinghai yellow chickens (3 slow-growing chickens and 3 fast-growing chickens) to collected leg muscles. Total RNAs were isolated with Trizol (TIANGEN, Beijing, China) and miRNAs were reverse transcribed into cDNA with the miRNA First-Strand cDNA kit (TIANGEN, Beijing, China). The forward primers used for quantification in the study were designed using Primer 5.0 and U6 small nuclear RNA (U6) was used for the housekeeping gene. The qPCR was conducted on QuantStudio 3 with the miRNA qPCR kit (TIANGEN, Beijing, China), and the reverse primers also came from the qPCR kit. The relative expression of miRNAs was calculated using the $2^{-\Delta\Delta CT}$ method (Rao et al., 2013).

Isolation, Culture and Identification of Chicken Primary Myoblasts (CPMs)

Chicken primary myoblasts (CPMs) were isolated from the leg muscle of 12-day-old chicken embryos according to Zhang et al. (2020b). The bones and blood clots in the muscles were separated, and the muscles were cut into meat sludge in a 10 cm sterile petri dish using medical scissors. The muscle was digested with collagenase type I (Gibco, Grand Island, NY) at 37°C to obtain single cells. The cell suspension after digestion was filtered, and then cultured in a 10 cm cell culture dish. CPMs were cultured in DMEM/F12 medium (Hyclone, UT) supplemented with 20% fetal bovine serum (Gibco, Grand Island) and 1% penicillin/streptomycin solution (Sangon Biotech, Shanghai, China). The differentiation of CPMs was induced by DMEM/F12 medium (Hyclone, UT) supplemented with 2% horse serum (Solarbio, Beijing, China) and 1% penicillin/streptomycin solution (Sangon Biotech, Shanghai, China) (Li et al., 2018; Li et al., 2019).

The purity of CPMs was identified by immunofluorescence. When seeded CPMs on the 6-well plates grew to 90%, media was removed and cells were washed twice gently with PBS (Hyclone, UT). Cells were fixed in 4% formaldehyde (Solarbio, Beijing, China) for 30 min. Hence treated with 0.5% Triton X-100 (Solarbio, Beijing, China) for 20 min, blocked with 5% goat serum (Solarbio, Beijing, China) for 30 min at 37°C, then incubated with anti-Desmin antibody (1:500, Bioss, Beijing, China) for 2 h at 37°C. After washing with PBST 3 times, the cells were incubated with DylLight 594 Conjugated AffiniPure Goat Anti-rabbit IgG (1:500, BOSTER, CA). Cell nuclei were stained with DAPI (Beyotime, Shanghai, China) for 1 min at room temperature. Fluorescent inverted microscope (DMi 8, Leica, Germany) is used to photograph these cells. Finally, Image Pro Plus (6.0) software is used to count positive cells (Desmin) and total cells (DAPI) numbers respectively.

Effect Exploration of miR-24-3p on Proliferation and Differentiation of CPMs

Transfections were performed with jetPRIME Reagent (Polyplus, Illkirch, France), with 60 nM miR-24-3p mimic and mimic NC (GenePharma, Shanghai, China) or 100 nM miR-24-3p inhibitor and inhibitor NC (GenePharma, Shanghai, China).

The cell counting kit-8 (CCK-8, Vazyme, Nanjing, China) and 5-ethynyl-2'-deoxyuridine (**EdU**) assay kit (RIBOBIO, Guangzhou, China) were used to detect cell proliferation in the 48-well plates. After transfection, we measured the absorbance at 450 nm for cells at 0, 12, 24, 36, and 48 h using the CCK-8 solution on the microplate reader (Perkin Elmer, MA). The EdU test was performed 24 h after transfection. Fluorescent inverted microscope (DMi 8, Leica, Germany) is used to photograph these cells. Finally, Image Pro Plus (6.0) software is used to count positive cells (EdU) and total cells (Hoechst) numbers respectively.

When CPMs seeded in a 12-well plate grew to 90%, they were transfected and induced to differentiate. After 48 h, we stained myotubes with the immunofluorescence method, which was same as that of Desmin staining described above. Finally, Image Pro Plus (6.0) software is used to calculate the areas of positive cells (Desmin) and total cells (DAPI) respectively.

Total RNAs were extracted from the proliferation or differentiation cells with Trizol (TIANGEN, Beijing, China). First strand cDNA was synthesized with HiScript II Q RT SuperMix kit (Vazyme, Nanjing, China) and ChamQTM SYBR qPCR Master Mix kit (Vazyme, Nanjing, China) was used for real-time quantitative PCR (**qPCR**). Expression of proliferation-related gene P21 and differentiation-related genes (MYOD, MYOG and MYHC) were detected with ACTB used as the housekeeping gene. Sequences of primers were shown in Table S1 and they were synthesized by Sangon Biotech Co., Ltd (Shanghai, China).

Statistical Analysis for Cell Experiment Results

Significance analysis was performed using SPSS13.0 software with the method Independent-Samples T-Test between 2 groups. The data were considered statistically significant with $P \leq 0.05$ (*), $P \leq 0.01$ (**), or $P \leq 0.001$ (***). All data were presented as means $\pm$ standard deviation (**SD**).

RESULTS

Phenotype Comparison of the Slow- and Fast-Growing Groups

The average live weight of the slow- and fast-growing groups were 1353.33 ± 14.53 (g) and 2553.33 ± 97.31 (g), and the average leg muscle weight were 94.27 ± 2.27 (g) and 182.73 ± 10.74 (g). Significance was analyzed between the slow- and fast-growing groups with the method independent sample T-test in SPSS 13.0. The results showed that there were significant differences between the 2 groups for live weight ($P = 0.000$) and leg muscle weight ($P = 0.012$).

RNA Sequence

Results of data quality control and comparative analysis were shown in Table S2. Raw reads were more than 9254587 (S_1) in each sample. Clean data (clean reads) were obtained by removing Containing 'N' reads and reads with Length <18 or Length >30. The proportion of clean reads was above 84.18% (F_4). The percentage of clean reads with Q30 was more than 86.17% (F_5). The comparative analysis showed that the proportion of mapped reads were all more than 65.67% (F_6).

Differential Expression Analysis and Target Gene Functional Annotation

In this study, a total of 651 miRNAs were identified, including 344 known miRNAs and 307 newly predicted miRNAs. Twelve differentially expressed miRNAs (DEMs) were obtained with the standard $P \leq 0.05$ (Table S3). There were 6 up-regulated (novel_miR_133, novel_miR_318, novel_miR_151, novel_miR_304, novel_miR_174, novel_miR_302) and 6 down-regulated DEMs (gga-miR-1416-5p, gga-miR-338-5p, gga-miR-100-5p, gga-miR-30a-3p, gga-miR-460b-5p, gga-miR-24-3p) in the fast-growing group compared to the slow-growing group (Table S3 and Figure 1a). The hierarchical clustering analysis showed that samples in the same group clustered together (Figure 1b).

A total of 150 target genes were predicted for the DEMs (Table S4). The first column is the name of DEMs, the third column is the sequence of DEMs, and the second column is the target gene ID of DEMs. Because miRNAs affected biological functions by regulating target genes, we analyzed the target genes for functional enrichment.

The GO enrichment analysis of the target genes was performed and a total of 148 significantly enriched GO terms were obtained with $P \leq 0.05$. There were 132 biological process (**BP**) terms, 8 cellular component (**CC**)
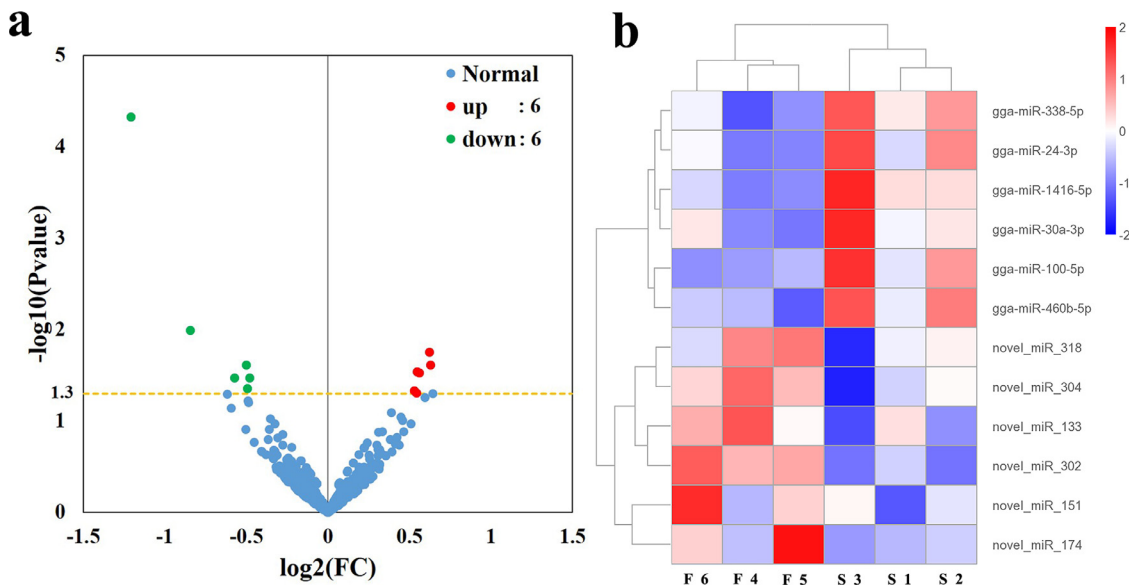
Figure 1. Analysis of DEMs. **(a)** The volcano plot of DEMs. **(b)** Hierarchical clustering analysis of DEMs. DEMs: differentially expressed miRNAs, FC: fold change, Blue: low expression, Red: high expression
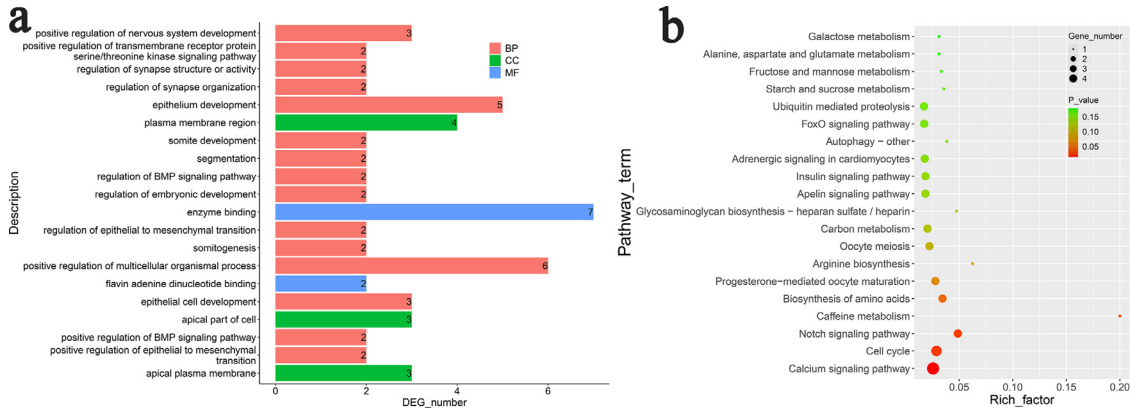
Figure 2. Enrichment analysis for target genes of DEMs. (a) The 20 top enriched GO terms. (b) The top 20 KEGG pathways. BP: biological process, CC: cellular component, MF: molecular function. The *P* values of GO terms and KEGG pathways decrease from top to bottom.

terms and 8 molecular function (**MF**) terms. Classification histogram was constructed for the first 20 GO terms (Figure 2a) and the BP terms in top 20 are listed in Table 1. Most of these items are related to growth and development, such as positive regulation of epithelial to mesenchymal transition, positive regulation of BMP signaling pathway, epithelial cell development, epithelium development and regulation of synapse organization, etc. The target genes of miR-24-3p and novel_miR_133 were most frequently enriched in these items, suggesting that these 2 miRNAs play an important role.

The KEGG pathway analysis of the target genes was performed and the top 20 pathways were shown in Figure 2b. Among them, 5 pathways were significantly enriched ($P \leq 0.05$). These include the calcium signaling pathway, cell cycle, notch signaling pathway, caffeine metabolism, and biosynthesis of amino acids (Table 2).

The target genes of miR-24-3p and novel_miR_133 are enriched most frequently in these pathways. Some pathways in the first 20 are closely related to growth and development, including carbon metabolism, insulin signaling pathway, and FoxO signaling pathway, etc.

Analysis of Hub Genes and miRNAs

We used the plug-in Cytohubba in the Cytoscape (3.6.1) to find the top 20 hub genes with the Maximal Clique Centrality (**MCC**) method (Table 3). The hub genes are important nodes in biological networks (Chin et al., 2014). The higher the value of MCC, the more important the gene is considered. The target genes of novel_miR_133 and miR-24-3p account for the most largest proportion in the top 20 hub genes.

Table 1. The Significantly enriched biological process items in the top 20 GO terms.

Term ID	Term name	*P*-value	Target gene name	miRNAs
GO:0010718	Positive regulation of epithelial to mesenchymal transition	0.003	NOTCH1; CRB2	gga-miR-24-3p; novel_miR_133
GO:0030513	Positive regulation of BMP signaling pathway	0.003	NOTCH1; CRB2	gga-miR-24-3p; novel_miR_133
GO:0002064	Epithelial cell development	0.005	HYDIN; NOTCH1; ROS1	novel_miR_151; gga-miR-24-3p; gga-miR-460b-5p
GO:0051240	Positive regulation of multicellular organismal process	0.007	ACE2; RBM19; ANAPC2; NOTCH1; CRB2; CAPRIN1	novel_miR_133; gga-miR-460b-5p; novel_miR_133; gga-miR-24-3p; novel_miR_133; gga-miR-24-3p
GO:0001756	Somitogenesis	0.008	NOTCH1; CRB2	gga-miR-24-3p; novel_miR_133
GO:0010717	Regulation of epithelial to mesenchymal transition	0.009	NOTCH1; CRB2	gga-miR-24-3p; novel_miR_133
GO:0045995	Regulation of embryonic development	0.009	RBM19; NOTCH1	gga-miR-460b-5p; gga-miR-24-3p
GO:0030510	Regulation of BMP signaling pathway	0.010	NOTCH1; CRB2	gga-miR-24-3p; novel_miR_133
GO:0035282	Segmentation	0.012	NOTCH1; CRB2	gga-miR-24-3p; novel_miR_133
GO:0061053	Somite development	0.012	NOTCH1; CRB2	gga-miR-24-3p; novel_miR_133
GO:0060429	Epithelium development	0.013	HYDIN; PODXL; NOTCH1; CRB2; ROS1	novel_miR_151; novel_miR_133; gga-miR-24-3p; novel_miR_133; gga-miR-460b-5p
GO:0050803	Regulation of synapse structure or activity	0.013	CAPRIN1; ANAPC2	gga-miR-24-3p; novel_miR_133
GO:0050807	Regulation of synapse organization	0.013	CAPRIN1; ANAPC2	gga-miR-24-3p; novel_miR_133
GO:0090100	Positive regulation of transmembrane receptor protein serine/threonine kinase signaling pathway	0.016	NOTCH1; CRB2	gga-miR-24-3p; novel_miR_133
GO:0051962	Positive regulation of nervous system development	0.017	CAPRIN1; ANAPC2; NOTCH1	gga-miR-24-3p; novel_miR_133; gga-miR-24-3p

Note: Target genes and miRNAs in the table are corresponding.

Table 2. The significantly enriched KEGG pathways.

KEGG pathway ID	KEGG pathway name	P-value	Target gene name	miRNAs
gga04020	Calcium signaling pathway	0.015	ATP2B4; RYR3; ERBB4; RYR2	gga-miR-24-3p; gga-miR-24-3p; novel_miR_133; novel_miR_304
gga04110	Cell cycle	0.025	CREBBP; ANAPC1; ANAPC2	novel_miR_133; gga-miR-24-3p; novel_miR_133
gga04330	Notch signaling pathway	0.027	CREBBP; NOTCH1	novel_miR_133; gga-miR-24-3p
gga00232	Caffeine metabolism	0.035	XDH	novel_miR_133
gga01230	Biosynthesis of amino acids	0.049	PHGDH; ASS1	gga-miR-24-3p; gga-miR-460b-5p

Note: Target genes and miRNAs in the table are corresponding.

Finally, the combined results of GO and KEGG analysis suggest that novel_miR_133 and miR-24-3p are the key miRNAs for the skeletal muscle, and miR-24-3p was selected for additional functional investigation in chicken primary myoblasts.

Validation of DEMs by qPCR

We selected six DEMs for comparison groups of slow- and fast-growing chicken by qPCR (Figure 3). Red columns represent TPM of miRNA-seq and green columns represent relative expression of qPCR. The result of qPCR was highly consistent with that of miRNA-seq in slow- and fast-growing groups.

Results of Purity, Transfection Efficiency, and Interference Efficiency for CPMs

The purity of CPMs was analyzed with the immunofluorescence method. Desmin and DAPI staining were performed when the cells grew to 80% and 4 biological replicates were set up in a 12-well plate (Figure 4a). The average percentage of Desmin positive cells was as high as 93.99% by software Image Pro Plus (6.0), which indicated that CPMs had high purity and could be used for subsequent experiments. Mimic NC and inhibitor NC labeled by FAM were used to transfect CPMs, and then the white light field (Bright) and fluorescence field (FAM) were photographed to observe the transfection

Table 3. The top 20 hub genes.

node_name	MCC	miRNA
COL6A2	27	novel_miR_133
COL5A2	26	novel_miR_133
COL5A1	25	novel_miR_133
COL4A3	24	novel_miR_133
COL4A4	24	novel_miR_133
CTNNB1	11	gga-miR-24-3p
NOTCH1	9	gga-miR-24-3p
CREBBP	8	novel_miR_133
FOXO1	7	novel_miR_304
GCK	5	novel_miR_133
MEP1A	4	novel_miR_133
RRP9	4	novel_miR_304
NOP14	4	gga-miR-460b-5p
MDN1	3	novel_miR_133
RBM19	3	gga-miR-460b-5p
ELL	3	gga-miR-24-3p
ANAPC1	3	gga-miR-24-3p
FOXN3	2	gga-miR-24-3p
COL11A1	2	novel_miR_133
SKIV2L	2	gga-miR-24-3p

efficiency. Figure 4b shows that mimic NC and inhibitor NC were successfully transfected into CPMs. The overexpression and interference efficiency of miR-24-3p were detected by qPCR 24 h after transfection with miR-24-3p mimic and mimic NC or miR-24-3p inhibitor and inhibitor NC. The results showed that the expression of miR-24-3p was significantly increased when CPMs were transfected with mimic (Figure 4c), while it was significantly down-regulated when transfected with inhibitor (Figure 4d).

miR-24-3p Inhibits the Proliferation of CPMs

When proliferating CPMs were transfected with miR-24-3p mimic, the relative expression detected by qPCR of cyclin dependent kinase inhibitor 1A (**P21**) was significantly up-regulated (Figure 5a). While transfection with miR-24-3p inhibitor had the opposite effect (Figure 5b).

In addition, The CCK-8 and EdU assay kit were used to detect cell proliferation in the 48-well plates. Results showed the absorbance at 450 nm decreased significantly when cells transfected with mimic after 24 h (Figure 5c). However, transfection with inhibitor significantly increased the absorbance after 12 h (Figure 5d). The EdU assay showed the ratio of proliferative cells (cell numbers of EdU/cell numbers of Hoechst) in the miR-24-3p mimic group was significantly reduced compared with the mimic NC group (Figure 5e and g). Conversely, after inhibition of miR-24-3p, the ratio of cells in proliferation significantly increased (Figure 5f and h). These results suggest that miR-24-3p inhibits proliferation of CPMs.

miR-24-3p Promotes the Differentiation of CPMs

When CPMs were transfected and simultaneously induced to differentiate, the expression of MYOD, MYOG, and MYHC were detected by qPCR after 48 h. Overexpression of miR-24-3p significantly up regulated the mRNA expression of the 3 differentiation marker genes (Figure 6a), while inhibition of miR-24-3p had the opposite effect (Figure 6b). Moreover, the immunofluorescence staining showed that overexpression of miR-24-3p significantly promoted the formation of myotubes (Figure 6c and e), while inhibition of miR-24-3p significantly reduced the area of myotubes (Figure 6d and f). Overall, the results suggested that miR-24-3p promotes differentiation of CPMs.
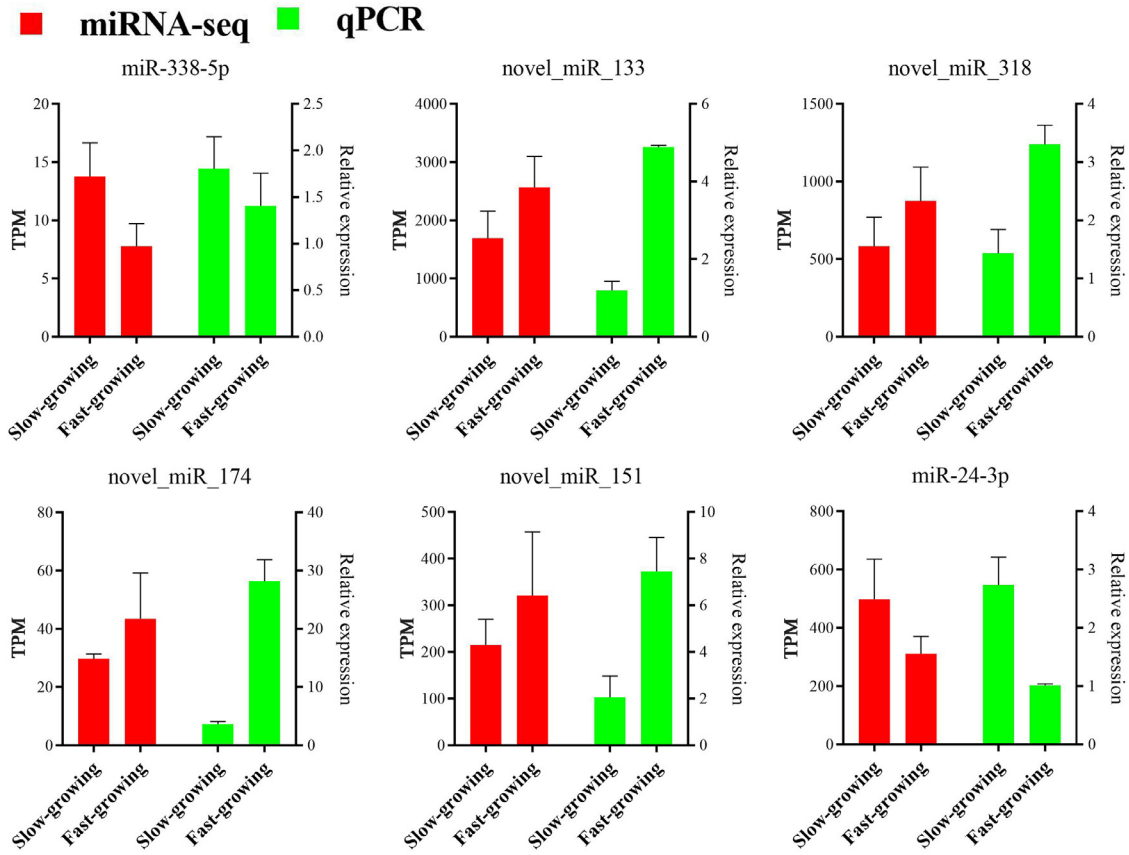
Figure 3. Expression level of six DEMs detected by miRNA-seq and qPCR. Red columns represent miRNA-seq results and green columns represent qPCR results. TPM, Transcripts Per Million.
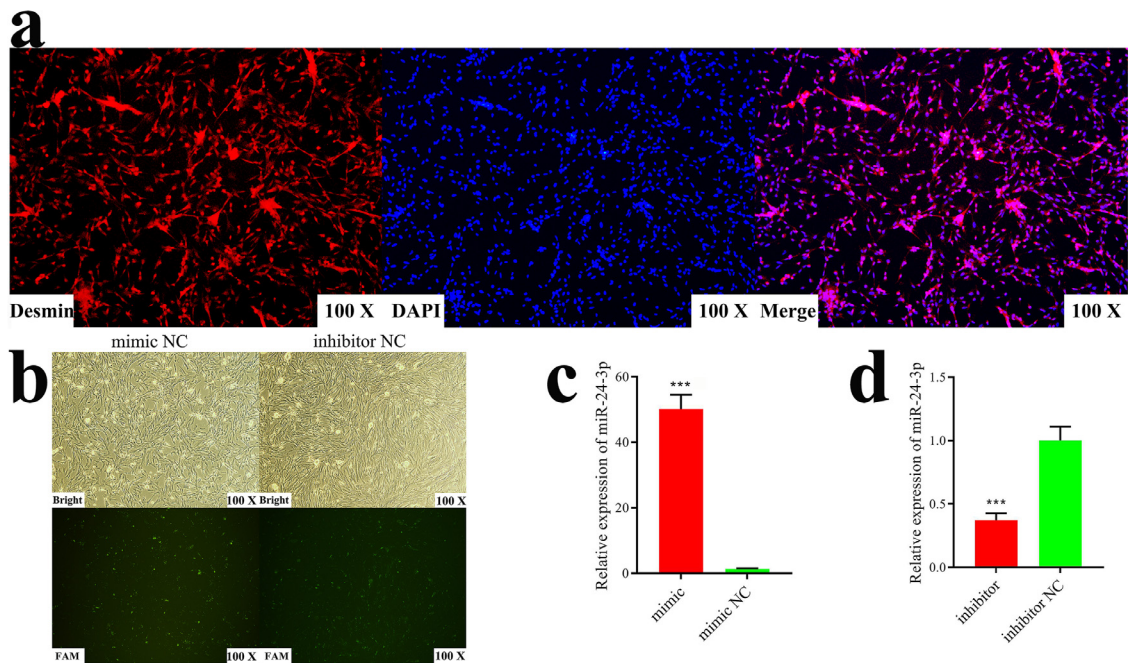
Figure 4. Purity identification and transfection efficiency for CPMs. (a) Immunofluorescence staining of Desmin for CPMs. (b) Transfected cells with mimic NC and inhibitor NC photographed by fluorescence inverted microscope. (c, d) Relative expression of miR-24-3p detected by qPCR after transfected with miR-24b-3p mimic or inhibitor in CPMs. The results are shown as the Mean ± SD of 4 independent experiments. ***$P < 0.001$.
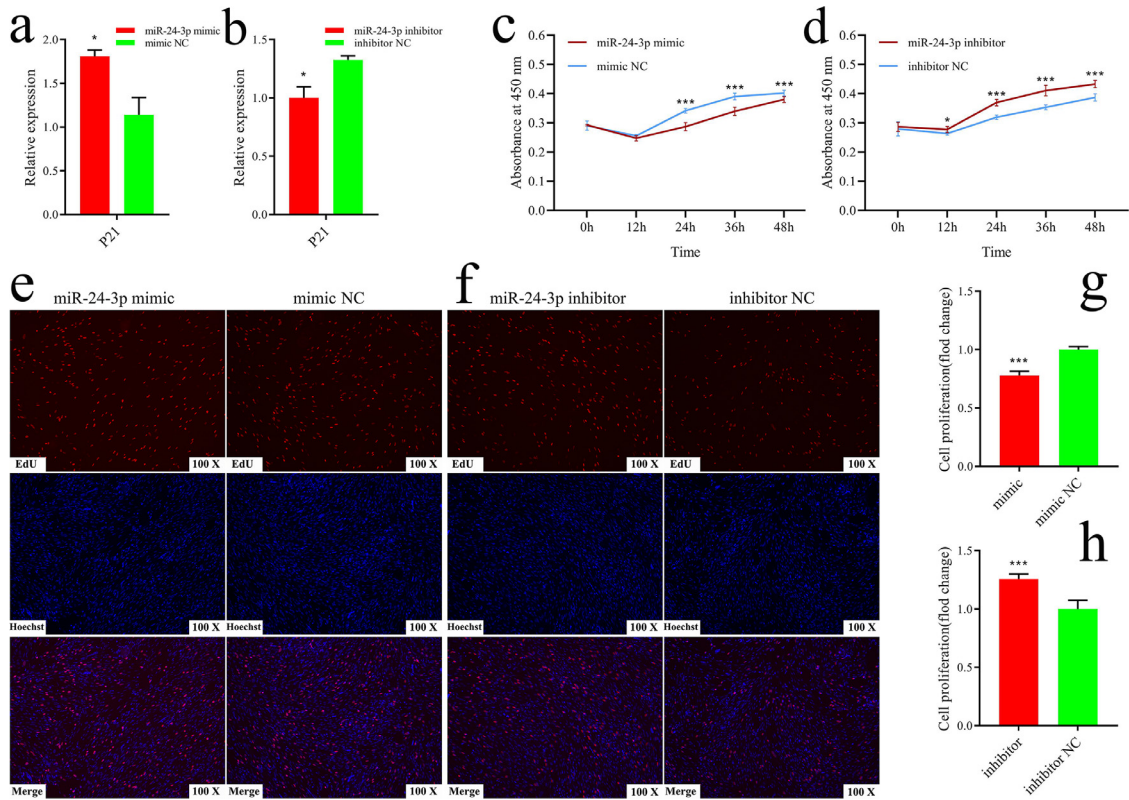
Figure 5. miR-24-3p inhibits the proliferation of CPMs. (a, b) Relative expression of P21 detected by qPCR after transfected with miR-24-3p mimic or inhibitor in CPMs. (c, d) Absorbance detection at 450 nm in CPMs at 0 h, 12 h, 24 h, 36 h, 48 h after overexpression or inhibition of miR-24-3p. (e, f) EdU staining of CPMs after transfection of miR-24-3p mimic or inhibitor. (g, h) The fold change of proliferation rates calculated by Image Pro Plus (6.0) software according to EdU and Hoechst staining images. The results are shown as the Mean ± SD of 3 independent experiments. $*P < 0.05$, $***P < 0.001$.
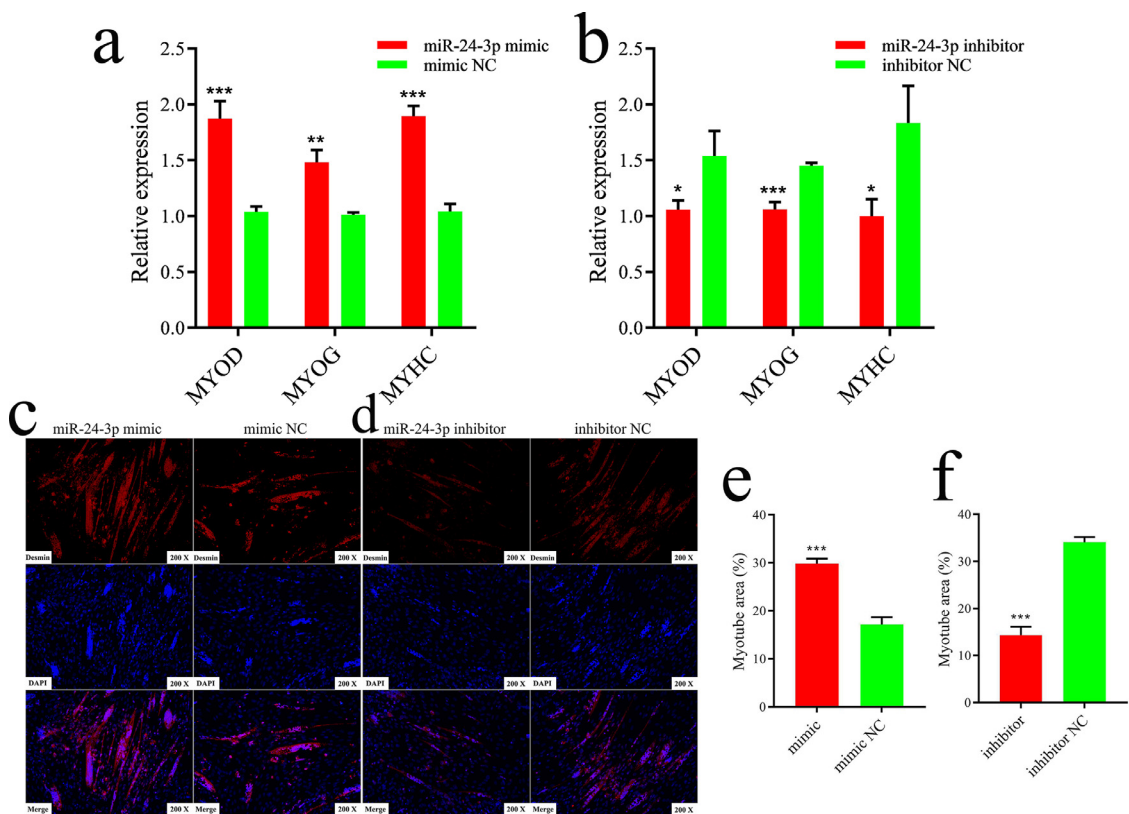
Figure 6. miR-24-3p promotes the differentiation of CPMs. (a, b) Relative expression detected by qPCR of three differentiation marker genes (MYOD MYOG and MYHC) after transfection of miR-24-3p mimic or inhibitor. (c, d) Desmin staining of differentiated CPMs at 48 h after transfected with miR-24b-3p mimic or inhibitor. (e, f) Myotube area (%) of CPMs calculated by Image Pro Plus (6.0) software according to Desmin and DAPI staining images. The results are shown as the Mean ± SD of 3 independent experiments. $*P < 0.05$, $**P < 0.01$, $***P < 0.001$.

DISCUSSION

Chicken meat provides a large amount of high-quality protein for human beings (Ren, et al., 2018), in which skeletal muscle plays a major role. Therefore, the growth and development of skeletal muscle have always been a focus of the broiler industry (Saneyasu, et al., 2017). Yellow-feathered broilers are especially popular in China in recent years (Jiang, et al., 2018) because of their better meat quality (Jiang, et al., 2019; Wang, et al., 2019). However, their growth rate and meat production rate are low. miRNAs were found play an important role in the growth of chicken (Vishnoi and Rani, 2017) and their regulation mechanism is still unclear.

In this study, we collected the leg muscles of slow- and fast-growing female Jinghai yellow chickens and finally identified two important miRNAs novel_miR_133 and miR-24-3p with miRNA-seq. Novel_miR_133 was a newly identified miRNA in the study. GO and KEGG analysis showed that target genes of novel_miR_133 covered most of the top 20 terms. Many target genes are indispensable and play an important role in the growth of skeletal muscles, such as CRB2, CREBBP, ERBB4, COL5A1, COL5A2, COL6A2, COL4A3, and COL4A4.

The cell cycle checkpoint mediator CRB2 is essential for the cellular response to DNA damage and repair (Kilkenny et al., 2008). CRB2 is a hub gene in the gene co-expression network for chickens, and was also found to be significantly up-regulated in the skeletal muscle under both acute and chronic heat stress stages (Srikanth et al., 2019). Another target gene CREBBP (CBP) was discovered to positively influence myogenesis in C2C12 cells (Sartorelli et al., 1997; Polesskaya et al., 2001). Recent research in mice has also shown that CREBBP is required for the control and maintenance of contractile function and transcriptional homeostasis in skeletal muscle and, ultimately, organism survival (Svensson et al., 2020). ERBB4 is a receptor, which can mediate the function of most proteins with an EGF-like domain (Segers and Dugaucquier, 2020). Ennequin et al. (2015) and Paatero et al. (2019) have confirmed the importance of ERBB4-mediated signaling pathway in muscle development for zebrafish and mice. Collagens, which account for about one-third of the total protein in the postnatal animal, are the largest and most abundant proteins in the body (Li and Wu, 2018). They comprise 28 protein types that contain at least one triple-helical domain and interact with cells via several receptor families and regulate their proliferation, migration, and differentiation (Hennet, 2019; Ricard-Blum, 2011). Collagens have been found to play an important role in the structural maintenance and normal development of skeletal muscle (Tam et al., 2015; Baumert et al., 2018; Mohammadkhah et al., 2018). Our results showed that 7 members of the collagen family were predicted for novel_miR_133, and the mRNA and miRNA expression networks showed that 5 (COL4A3, COL4A4, COL5A1, COL5A2, and COL6A1) were in the core position, further illustrating the importance of this gene family in skeletal muscle.

As a tumor suppressor miRNA, miR-24-3p has been widely studied in a variety of cancers, such as nasopharyngeal carcinoma (Ye et al., 2016), lung cancer (Yan et al., 2018), and breast cancer (Khodadadi-Jamayran, et al., 2018). In recent years, miR-24-3p has also been found to be related to growth and development. In 2019, Hu et al. (2019) found that bta-miR-24-3p could promote myogenic differentiation but inhibited proliferation by directly targeting and suppressing ACVR1B expression in myogenic progenitor cells of bovine. Holstein et al. (2020) found miR-24-3p could promote C2C12 differentiation via 3'UTR-mediated MRTF-A repression. We found its downstream target genes closely related to growth and development, including Notch1, CTNNB1, and RYR3.

Notch1 is a member of the Notch signaling pathway, which is an evolutionarily conserved developmental network critical for embryonic and postnatal regulation of tissue growth, homeostasis, and repair (Conti et al., 2016). Studies have shown that Notch1 and Notch2 coordinately maintain the stem-cell pool in the quiescent state by preventing activation and regulate stem-cell-fate decision in the activated state, governing adult muscle regeneration (Fujimaki et al., 2018). In our experiment, Notch1 was enriched in the most BP entries of the top 20 GO terms. KEGG pathway analysis showed that the Notch signaling pathway was also significantly enriched and the gene was among the top 20 hub genes.

CTNNB1 (β-catenin) is a key regulatory molecule of the Wnt signaling pathway. The pathway is important for tissue homeostasis and regulation of cell proliferation, differentiation, and function (Agaimy and Haller, 2016). Previous studies have shown that CTNNB1 could promote C2C12 differentiation (Figeac and Zammit, 2015; Cui et al., 2019; Han, et al., 2019). In a recent study, Zhang et al. (2020a) found that the Wnt/β-catenin signaling pathway could regulate the atrophy of skeletal muscle for chicken.

RYR3 is one isoform of ryanodine receptors (**RyRs**), which are ubiquitous intracellular calcium (Ca^{2+}) release channels (Santulli et al., 2018). RYR1 is predominantly expressed in muscle, while RYR3 is predominantly expressed in cardiac and brain tissues in mammals (Ottini et al., 1996). Interestingly, the 2 isoforms were found to be expressed almost equally in the muscle of birds, fish and other non-mammals (Murayama and Kurebayashi, 2011; Ottini et al., 1996). RYR3 is expressed in developing zebrafish muscle, and is required for normal locomotive behaviors by modifying the functions of other RyR channels (Chagovetz et al., 2019). Chiang et al. (2007) found that SNPs of βRYR could affect the amount of Ca^{2+} release and thus affected calcium channel activity in the study of turkey skeletal muscle. Sporer et al. (2012) speculated that RYR3 (βRYR) could regulate PSE breast meat with RYR1 by controlling Ca^{2+} release in turkeys. In the present, RYR3 was enriched in the calcium signaling pathway, which is the most significant pathway. In addition, other important genes, such as MYO18A and PHGDA, were also predicted.

From the results for miR-24-3p, we speculated that it might also play an important role in the development of chicken skeletal muscle. Therefore, we explored the effects of miR-24-3p on the proliferation and differentiation of CPMs.

In the experiment of miR-24-3p on the proliferation of CPMs, we found that the expression of P21 significantly increased in the miR-24-3p mimic group, while decreased in the group with miR-24-3p inhibitor. It is well known that P21 could inhibit cell proliferation (Massagué, 2004). Both the EdU and CCK-8 assays showed that CPMs proliferation was inhibited when cells were transfected with miR-24-3p mimic, while the ratio of cells in proliferation increased when CPMs were treated with miR-24-3p inhibitor. This inhibition by miR-24-3p is similar to the result of Hu et al. (2019) in bovine myogenic progenitor cells for miR-24-3p.

During the differentiation of CPMs, we found that overexpression of miR-24-3p significantly up-regulated expression of MYOD, MYOG and MYHC. Expression of these 3 differentiation marker genes was down-regulated after transfection with inhibitor. MYOD, MYOG, and MYHC could promote and maintain the process of myoblast differentiation (Huang et al., 2019). This result preliminarily suggests that miR-24-3p promotes the differentiation of CPMs. Immunofluorescence staining of myotubes showed that overexpression of miR-24-3p significantly promoted the formation of myotubes. These results suggested that miR-24-3p promoted the differentiation of CPMs, similar to the effects of miR-24-3p on bovine myogenic progenitor cells (Hu et al., 2019) and C2C12 cells (Holstein et al., 2020). Compared with the function of miR-24-3p in other species, we infered that its role might be highly conserved among species.

Taken together, this study revealed 12 DEMs between slow- and fast-growing Jinghai yellow chickens and comprehensive analysis identified 2 miRNAs (novel_-miR_133 and miR-24-3p) closely related to the growth and development. Finally, we showed that miR-24-3p inhibited proliferation and promoted differentiation of CPMs. Our research provides a theoretical basis for the mechanism of skeletal muscle development for chickens through the regulation of miRNAs.

ACKNOWLEDGMENTS

DISCLOSURES

All authors declare that they have no competing interests.

SUPPLEMENTARY MATERIALS

Supplementary material associated with this article can be found in the online version at doi:10.1016/j.psj.2022.102120.

REFERENCES

Agaimy, A., and F. Haller. 2016. CTNNB1 (β-Catenin)-altered neoplasia: a review focusing on soft tissue neoplasms and parenchymal lesions of uncertain histogenesis. Adv. Anat. Pathol. 23:1–12.

Baumert, P., C. E. Stewart, M. J. Lake, B. Drust, and R. M. Erskine. 2018. Variations of collagen-encoding genes are associated with exercise-induced muscle damage. Physiol. Genomics. 50:691–693.

Betel, D., M. Wilson, A. Gabow, D. S. Marks, and C. Sander. 2008. The microRNA.org resource: targets and expression. Nucleic Acids Res. 36:D149–D153.

Cao, X., S. Tang, F. Du, H. Li, X. Shen, D. Li, Y. Wang, Z. Zhang, L. Xia, Q. Zhu, and H. Yin. 2020. miR-99a-5p Regulates the proliferation and differentiation of skeletal muscle satellite cells by targeting MTMR3 in chicken. Genes (Basel) 11:369.

Chagovetz, A. A., D. Klatt Shaw, E. Ritchie, K. Hoshijima, and D. J. Grunwald. 2019. Interactions among ryanodine receptor isotypes contribute to muscle fiber type development and function. Dis. Models Mech. 13:dmm038844.

Chiang, W., H. J. Yoon, J. E. Linz, J. A. Airey, and G. M. Strasburg. 2007. Divergent mechanisms in generating molecular variations of alphaRYR and betaRYR in turkey skeletal muscle. J. Muscle Res. Cell Motil. 28:343–354.

Chin, C. H., S. H. Chen, H. H. Wu, C. W. Ho, M. T. Ko, and C. Y. Lin. 2014. cytoHubba: identifying hub objects and sub-networks from complex interactome. BMC Syst. Biol. 8(Suppl 4):S11.

Conti, B., K. K. Slemmons, R. Rota, and C. M. Linardic. 2016. Recent insights into notch signaling in embryonal rhabdomyosarcoma. Curr. Drug Targets. 17:1235–1244.

Correia de Sousa, M., M. Gjorgjieva, D. Dolicka, C. Sobolewski, and M. Foti. 2019. Deciphering miRNAs' action through miRNA editing. Int. J. Mol. Sci. 20:6249.

Cui, S., L. Li, R. T. Yu, M. Downes, R. M. Evans, J. A. Hulin, H. P. Makarenkova, and R. Meech. 2019. β-Catenin is essential for differentiation of primary myoblasts via cooperation with MyoD and α-catenin. Development. 146:dev167080.

Ennequin, G., N. Boisseau, K. Caillaud, V. Chavanelle, M. Gerbaix, L. Metz, M. Etienne, S. Walrand, A. Masgrau, C. Guillet, D. Courteix, A. Niu, Y. P. Li, F. Capel, and P. Sirvent. 2015. Exercise training and return to a well-balanced diet activate the neuregulin 1/ErbB pathway in skeletal muscle of obese rats. J. Physiol. 593:2665–2677.

Figeac, N., and P. S. Zammit. 2015. Coordinated action of Axin1 and Axin2 suppresses β-catenin to regulate muscle stem cell function. Cell Signal. 27:1652–1665.

Franceschini, A., D. Szklarczyk, S. Frankild, M. Kuhn, M. Simonovic, A. Roth, J. Lin, P. Minguez, P. Bork, C. von Mering, and L. J. Jensen. 2013. STRING v9.1: protein-protein interaction networks, with increased coverage and integration. Nucleic Acids Res. 41:D808–D815.

Friedländer, M. R., S. D. Mackowiak, N. Li, W. Chen, and N. Rajewsky. 2012. miRDeep2 accurately identifies known and hundreds of novel microRNA genes in seven animal clades. Nucleic Acids Res. 40:37–52.

Fu, S., Y. Zhao, Y. Li, and G. Li. 2018. Characterization of miRNA transcriptome profiles related to breast muscle development and intramuscular fat deposition in chickens. J. Cell. Biochem. 119:7063–7079.

Fujimaki, S., D. Seko, Y. Kitajima, K. Yoshioka, Y. Tsuchiya, S. Masuda, and Y. Ono. 2018. Notch1 and Notch2 coordinately regulate stem cell function in the quiescent and activated states of muscle satellite cells. Stem Cells 36:278–285.

Han, S., C. Cui, H. He, X. Shen, Y. Chen, Y. Wang, D. Li, Q. Zhu, and H. Yin. 2019. Myoferlin regulates Wnt/β-catenin signaling-mediated skeletal muscle development by stabilizing dishevelled-2 against autophagy. Int. J. Mol. Sci. 20:5130.

Hennet, T. 2019. Collagen glycosylation. Curr. Opin. Struct. Biol. 56:131–138.

Holstein, I., A. K. Singh, F. Pohl, D. Misiak, J. Braun, L. Leitner, S. Hüttelmaier, and G. Posern. 2020. Post-transcriptional regulation of MRTF-A by miRNAs during myogenic differentiation of myoblasts. Nucleic Acids Res 48:8927–8942.

Hu, X., Y. Xing, L. Ren, Y. Wang, Q. Li, X. Fu, Q. Yang, L. Xu, and L. Willems. 2019. Bta-miR-24-3p controls the myogenic differentiation and proliferation of fetal, bovine, skeletal muscle-derived progenitor cells by targeting ACVR1B. Animals (Basel) 9:859.

Huang, W., L. Guo, M. Zhao, D. Zhang, H. Xu, and Q. Nie. 2019. The inhibition on MDFIC and PI3K/AKT pathway caused by miR-146b-3p triggers suppression of myoblast proliferation and differentiation and promotion of apoptosis. Cells. 8:656.

Jebessa, E., H. Ouyang, B. A. Abdalla, Z. Li, A. Y. Abdullahi, Q. Liu, Q. Nie, and X. Zhang. 2018. Characterization of miRNA and their target gene during chicken embryo skeletal muscle development. Oncotarget. 9:17309–17324.

Jiang, S., H. K. El-Senousey, Q. Fan, X. Lin, Z. Gou, L. Li, Y. Wang, A. M. Fouad, and Z. Jiang. 2019. Effects of dietary threonine supplementation on productivity and expression of genes related to protein deposition and amino acid transportation in breeder hens of yellow-feathered chicken and their offspring. Poult. Sci. 98:6826–6836.

Jiang, S. Q., Z. Y. Gou, X. J. Lin, and L. Li. 2018. Effects of dietary tryptophan levels on performance and biochemical variables of plasma and intestinal mucosa in yellow-feathered broiler breeders. J. Anim. Physiol. Anim. Nutr. (Berl.) 102:e387–e394.

Kansal, R., R. K. Kanojia, V. Kumar, K. Vaiphei, and M. S. Dhillon. 2019. Role of PAX-7 as a tissue marker in mangled extremity: a pilot study. Eur. J. Orthop. Surg. Traumatol. 29:1131–1140.

Khodadadi-Jamayran, A., B. Akgol-Oksuz, Y. Afanasyeva, A. Heguy, M. Thompson, K. Ray, A. Giro-Perafita, I. Sánchez, X. Wu, D. Tripathy, A. Zeleniuch-Jacquotte, A. Tsirigos, and F. J. Esteva. 2018. Prognostic role of elevated mir-24-3p in breast cancer and its association with the metastatic process. Oncotarget. 9:12868–12878.

Kilkenny, M. L., A. S. Doré, S. M. Roe, K. Nestoras, J. C. Ho, F. Z. Watts, and L. H. Pearl. 2008. Structural and functional analysis of the Crb2-BRCT2 domain reveals distinct roles in checkpoint signaling and DNA damage repair. Genes Dev. 22:2034–2047.

Langmead, B., C. Trapnell, M. Pop, and S. L. Salzberg. 2009. Ultrafast and memory-efficient alignment of short DNA sequences to the human genome. Genome Biol. 10:R25.

Lee, R. C., R. L. Feinbaum, and V. Ambros. 1993. The C. elegans heterochronic gene lin-4 encodes small RNAs with antisense complementarity to lin-14. Cell. 75:843–854.

Li, B., V. Ruotti, R. M. Stewart, J. A. Thomson, and C. N. Dewey. 2010. RNA-Seq gene expression estimation with read mapping uncertainty. Bioinformatics 26:493–500.

Li, P., and G. Wu. 2018. Roles of dietary glycine, proline, and hydroxyproline in collagen synthesis and animal growth. Amino Acids. 50:29–38.

Li, T., G. Zhang, P. Wu, L. Duan, G. Li, Q. Liu, and J. Wang. 2018. Dissection of myogenic differentiation signatures in chickens by RNA-Seq analysis. Genes (Basel) 9:34.

Li, Z., B. Cai, B. A. Abdalla, X. Zhu, M. Zheng, P. Han, Q. Nie, and X. Zhang. 2019. LncIRS1 controls muscle atrophy via sponging

miR-15 family to activate IGF1-PI3K/AKT pathway. J. Cachexia Sarcopeni. 10:391–410.

Liu, B., J. Li, and M. J. Cairns. 2014. Identifying miRNAs, targets and functions. Briefings Bioinf. 15:1–19.

Liu, L. X., T. F. Dou, Q. H. Li, H. Rong, H. Q. Tong, Z. Q. Xu, Y. Huang, D. H. Gu, X. B. Chen, C. R. Ge, and J. J. Jia. 2016. Myostatin mRNA expression and its association with body weight and carcass traits in Yunnan Wuding chicken. Genet. Mol. Res. 15: gmr15048967.

Mao, X., T. Cai, J. G. Olyarchuk, and L. Wei. 2005. Automated genome annotation and pathway identification using the KEGG Orthology (KO) as a controlled vocabulary. Bioinformatics. 21:3787–3793.

Massagué, J. 2004. G1 cell-cycle control and cancer. Nature 432:298–306.

Mohammadkhah, M., P. Murphy, and C. K. Simms. 2018. Collagen fibril organization in chicken and porcine skeletal muscle perimysium under applied tension and compression. J. Mech. Behav. Biomed. Mater. 77:734–744.

Mok, G. F., R. H. Mohammed, and D. Sweetman. 2015. Expression of myogenic regulatory factors in chicken embryos during somite and limb development. J. Anat. 227:352–360.

Murayama, T., and N. Kurebayashi. 2011. Two ryanodine receptor isoforms in nonmammalian vertebrate skeletal muscle: possible roles in excitation-contraction coupling and other processes. Prog. Biophys. Mol. Biol. 105:134–144.

Ottini, L., G. Marziali, A. Conti, A. Charlesworth, and V. Sorrentino. 1996. Alpha and beta isoforms of ryanodine receptor from chicken skeletal muscle are the homologues of mammalian RyR1 and RyR3. Biochem. J. 315(Pt 1):207–216.

Ouyang, H., J. Yu, X. Chen, Z. Wang, and Q. Nie. 2020. A novel transcript of MEF2D promotes myoblast differentiation and its variations associated with growth traits in chicken. PeerJ. 8:e8351.

Paatero, I., V. Veikkolainen, M. Mäenpää, E. Schmelzer, H. G. Belting, L. J. Pelliniemi, and K. Elenius. 2019. ErbB4 tyrosine kinase inhibition impairs neuromuscular development in zebrafish embryos. Mol. Biol. Cell. 30:209–218.

Polesskaya, A., I. Naguibneva, L. Fritsch, A. Duquet, S. Ait-Si-Ali, P. Robin, A. Vervisch, L. L. Pritchard, P. Cole, and A. Harel-Bellan. 2001. CBP/p300 and muscle differentiation: no HAT, no muscle. EMBO J. 20:6816–6825.

Rao, X., X. Huang, Z. Zhou, and X. Lin. 2013. An improvement of the 2^(-delta delta CT) method for quantitative real-time polymerase chain reaction data analysis. Biostat. Bioinforma. Biomath. 3:71–85.

Reinhart, B. J., F. J. Slack, M. Basson, A. E. Pasquinelli, J. C. Bettinger, A. E. Rougvie, H. R. Horvitz, and G. Ruvkun. 2000. The 21-nucleotide let-7 RNA regulates developmental timing in Caenorhabditis elegans. Nature. 403:901–906.

Ren, T., Z. Li, Y. Zhou, X. Liu, R. Han, Y. Wang, F. Yan, G. Sun, H. Li, and X. Kang. 2018. Sequencing and characterization of lncRNAs in the breast muscle of Gushi and Arbor Acres chickens. Genome. 61:337–347.

Ricard-Blum, S. 2011. The collagen family. Cold Spring Harb. Perspect. Biol. 3:a004978.

Roelfsema, F., R. J. Yang, P. Y. Takahashi, D. Erickson, C. Y. Bowers, and J. D. Veldhuis. 2018. Effects of toremifene, a selective estrogen receptor modulator, on spontaneous and stimulated gh secretion, igf-i, and igf-binding proteins in healthy elderly subjects. J. Endocr. Soc. 2:154–165.

Saliminejad, K., H. R. Khorram Khorshid, S. Soleymani Fard, and S. H. Ghaffari. 2019. An overview of microRNAs: Biology, functions, therapeutics, and analysis methods. J. Cell. Physiol. 234:5451–5465.

Saneyasu, T., Y. Nakano, N. Tsuchii, A. Kitashiro, T. Tsuchihashi, S. Kimura, K. Honda, and H. Kamisoyama. 2019. Differential regulation of protein synthesis by skeletal muscle type in chickens. Gen. Comp. Endocrinol. 284:113246.

Saneyasu, T., T. Tsuchihashi, A. Kitashiro, N. Tsuchii, S. Kimura, K. Honda, and H. Kamisoyama. 2017. The IGF-1/Akt/S6 pathway and expressions of glycolytic myosin heavy chain isoforms are upregulated in chicken skeletal muscle during the first week after hatching. Anim. Sci. J. 88:1779–1787.

Santulli, G., D. Lewis, A. des Georges, A. R. Marks, and J. Frank. 2018. Ryanodine receptor structure and function in health and disease. Subcell. Biochem. 87:329–352.

Sartorelli, V., J. Huang, Y. Hamamori, and L. Kedes. 1997. Molecular mechanisms of myogenic coactivation by p300: direct interaction with the activation domain of MyoD and with the MADS box of MEF2C. Mol. Cell. Biol. 17:1010–1026.

Segers, V. F. M., and L. Dugaucquier. 2020. The role of ErbB4 in cancer. Cell. Oncol. (Dordr). 43:335–352.

Shi, J., and G. Sun. 2017. Effect of pre-miRNA-1658 gene polymorphism on chicken growth and carcass traits. Asian-Australas. J. Anim. Sci. 30:455–461.

Sporer, K. R., H. R. Zhou, J. E. Linz, A. M. Booren, and G. M. Strasburg. 2012. Differential expression of calcium-regulating genes in heat-stressed turkey breast muscle is associated with meat quality. Poult. Sci. 91:1418–1424.

Srikanth, K., H. Kumar, W. Park, M. Byun, D. Lim, S. Kemp, M. F. W. Te Pas, J. M. Kim, and J. E. Park. 2019. Cardiac and skeletal muscle transcriptome response to heat stress in kenyan chicken ecotypes adapted to low and high altitudes reveal differences in thermal tolerance and stress response. Front. Genet. 10:993.

Sun, G., F. Li, X. Ma, J. Sun, R. Jiang, Y. Tian, R. Han, G. Li, Y. Wang, and Z. Li. 2019. gga-miRNA-18b-3p inhibits intramuscular adipocytes differentiation in chicken by targeting the ACOT13 Gene. Cells 8:556.

Svensson, K., S. A. LaBarge, A. Sathe, V. F. Martins, S. Tahvilian, J. M. Cunliffe, R. Sasik, S. K. Mahata, G. A. Meyer, A. Philp, L. L. David, S. R. Ward, C. E. McCurdy, J. E. Aslan, and S. Schenk. 2020. p300 and cAMP response element-binding protein-binding protein in skeletal muscle homeostasis, contractile function, and survival. J. Cachexia Sarcopeni. 11:464–477.

Tam, C. S., J. E. Power, T. P. Markovic, C. Yee, M. Morsch, S. V. McLennan, and S. M. Twigg. 2015. The effects of high-fat feeding on physical function and skeletal muscle extracellular matrix. Nutr. Diabetes. 5:e187.

Trouten-Radford, L., X. Zhao, and B. W. McBride. 1991. IGF-I receptors in embryonic skeletal muscle of three strains of chickens selected for differences in growth capacity. Domest. Anim. Endocrinol. 8:129–137.

Vishnoi, A., and S. Rani. 2017. MiRNA biogenesis and regulation of diseases: an overview. Methods Mol. Biol. 1509:1–10.

Wang, H., X. Qin, S. Mi, X. Li, X. Wang, W. Yan, and C. Zhang. 2019. Contamination of yellow-feathered broiler carcasses: Microbial diversity and succession during processing. Food Microbiol. 83:18–26.

Wightman, B., I. Ha, and G. Ruvkun. 1993. Posttranscriptional regulation of the heterochronic gene lin-14 by lin-4 mediates temporal pattern formation in C. elegans. Cell. 75:855–862.

Yan, L., J. Ma, Y. Zhu, J. Zan, Z. Wang, L. Ling, Q. Li, J. Lv, S. Qi, Y. Cao, Y. Liu, L. Cao, Y. Zhang, Z. Qi, and L. Nie. 2018. miR-24-3p promotes cell migration and proliferation in lung cancer by targeting SOX7. J. Cell. Biochem. 119:3989–3998.

Ye, S. B., H. Zhang, T. T. Cai, Y. N. Liu, J. J. Ni, J. He, J. Y. Peng, Q. Y. Chen, H. Y. Mo, C. Jun, X. S. Zhang, Y. X. Zeng, and J. Li. 2016. Exosomal miR-24-3p impedes T-cell function by targeting FGF11 and serves as a potential prognostic biomarker for nasopharyngeal carcinoma. J. Pathol. 240:329–340.

Zhang, D. H., H. D. Yin, J. J. Li, Y. Wang, C. W. Yang, X. S. Jiang, H. R. Du, and Y. P. Liu. 2020a. KLF5 regulates chicken skeletal muscle atrophy via the canonical Wnt/β-catenin signaling pathway. Exp. Anim 69:430–440.

Zhang, G., F. Chen, P. Wu, T. Li, M. He, X. Yin, H. Shi, Y. Duan, T. Zhang, J. Wang, K. Xie, and G. Dai. 2020b. MicroRNA-7 targets the KLF4 gene to regulate the proliferation and differentiation of chicken primary myoblasts. Front. Genet. 11:842.